MESONS AND THE NUCLEON STRUCTURE *

A. SZCZUREK

Institute of Nuclear Physics,
Radzikowskiego 152, 31-342 Kraków, Poland

(Received October 9, 1996)

The nucleon light-cone wave function is expanded in terms of two-body meson-(bare baryon) Fock components. We find many interesting and surprising results for the flavour, spin and electromagnetic structure of the nucleon. The model leads to asymmetry of the light sea quarks which has important consequences for elementary Drell–Yan processes. We propose a further possibility to test this concept at HERA through the analysis of the structure of deep inelastic scattering (DIS) events induced by pion-exchange. Momentum and energy distributions of outgoing nucleons as well as rapidity and multiplicity distributions are investigated using Monte Carlo simulations. We investigate also possible consequences of the meson cloud in the nucleon for the production of W and Z bosons in the hadron–hadron collisions. A consistent analysis of deep-inelastic data and the gauge boson production data shows that the concept of virtual mesons in the nucleon is very useful in understanding the charged lepton asymmetry measured by the CDF collaboration at Fermilab. We critically study a possibility to test the $\bar{d}$–$\bar{u}$ asymmetry in the nucleon by the analysis of some asymmetries possible to measure in principle at RHIC.

PACS numbers: 14.40.-n, 14.20. Dh

1. Introduction

With the advent of high precision data on deep inelastic scattering, understanding of the nonperturbative flavour structure of the nucleon is becoming one of the pressing issues where the interests of particle and nuclear physics converge. It has been customarily assumed that the nucleon sea is flavor symmetric ($\overline{d}_p(x) = \overline{u}_p(x)$). There is no general principle that forces one to this hypothesis other than the fact that it appears as a natural consequence of a perturbative approach to the nucleon's parton distributions. At large Q^2 the perturbative QCD evolution is flavour independent and, to

* Presented at the "Meson 96" Workshop, Cracow, Poland, May 10–14, 1996.

leading order in log Q^2, generates equal number of $\bar{u}$ and $\bar{d}$ sea quarks. The $\bar{u}$–$\bar{d}$ asymmetry coming from effects of the interference between the u and d quarks from the perturbative sea $\bar{u}u$ and $\bar{d}d$ pairs and the valence u and d quarks of the nucleon was found to be negligible [1]. Perturbative QCD describes only the Q^2-evolution of deep inelastic structure functions, starting with certain nonperturbative input. There are no a priori reasons to expect a $\bar{u}$–$\bar{d}$ symmetric nonperturbative sea. Specifically, the observed [2] violation of the Gottfried Sum Rule (GSR)[3] provides experimental evidence that the nucleon sea is not flavour symmetric.

Furthermore, the strong correlations between quarks and antiquarks of the nonperturbative sea, exemplified by the pionic field in physical nucleons, leads to such an asymmetry [4–9]. The meson cloud model provides a natural explanation for the excess of $\bar{d}$ over $\bar{u}$ quarks already in its simplest form in which the proton contains components of a bare proton and π^0 and a bare neutron and π^+.

In this presentation I shall discuss the role of the meson cloud in deep-inelastic lepton scattering, especially in connection with the GSR, and for the dilepton production in the proton–proton collisions at high energies. This part of the presentation is an extension of our earlier works on the importance of the meson cloud in the nucleon for deep inelastic lepton-nucleon scattering [8, 9], Drell–Yan processes [10] and electromagnetic form factors [11]. I shall discuss also a structure of DIS events induced by the pion cloud and comment on the possibility to verify the concept of the pion cloud. In addition I shall comment on possible consequences of the meson cloud for the W and Z weak gauge boson production in the nucleon–(anti)nucleon collisions and confront the predictions with the existing CERN and FNAL experimental data. Finally I analyze whether a measurement of the W/Z production in proton–proton and proton–deuteron collisions could shed some new light on the $\bar{d}$–$\bar{u}$ asymmetry in the nucleon and in the consequence on the nucleon structure.

2. Meson cloud model of the nucleon and lepton deep inelastic scattering

In this model the nucleon is viewed as a quark core, termed a bare nucleon, 'surrounded' by the mesonic cloud. The nucleon wave function can be schematically written as a superposition of a few principle Fock components (only πN and $\pi\Delta$ are shown explicitly)

$$
\begin{aligned}
|p\rangle_{\text{phys}} = \sqrt{Z}\Big[\; & |p\rangle_{\text{core}} \\
& + \int dy\, d^2\vec{k}_\perp \phi_{N\pi}(y,\vec{k}_\perp)\Big(\sqrt{\frac{1}{3}}|p\pi^0; y, \vec{k}_\perp\rangle + \sqrt{\frac{2}{3}}|n\pi^+; y, \vec{k}_\perp\rangle\Big) \\
& + \int dy\, d^2\vec{k}_\perp \phi_{\Delta\pi}(y,\vec{k}_\perp) \\
& \times\Big(\sqrt{\frac{1}{2}}|\Delta^{++}\pi^-; y, \vec{k}_\perp\rangle - \sqrt{\frac{1}{3}}|\Delta^{+}\pi^{o}; y, \vec{k}_\perp\rangle + \sqrt{\frac{1}{6}}|\Delta^{o}\pi^+; y, \vec{k}_\perp\rangle\Big) \\
& + \dots\;\Big], \qquad (1)
\end{aligned}
$$

with Z being the wave function renormalization constant which can be calculated by imposing the normalization condition $\langle p|p\rangle = 1$. The $\phi(y, \vec{k}_\perp)'s$ are the light cone wave functions of the πN, $\pi\Delta$, *etc.* Fock states, y is the longitudinal momentum fraction of the π (meson) and $\vec{k}_\perp$ its transverse momentum.

The model includes all the mesons and baryons required in the description of the low energy nucleon–nucleon and hyperon-nucleon scattering, *i.e.*π, K, ρ, ω, K^* and N, Λ, Σ, Δ and Σ^*. The main ingredients of the model are the vertex coupling constants, the parton distribution functions for the virtual mesons and baryons and the vertex form factors which account for the extended nature of the hadrons. The coupling constants are assumed to be related via SU(3) symmetry which seems to be well established from low-energy hyperon-nucleon scattering.

It was suggested in Ref. [7] to use the light cone meson-baryon vertex form factor

$$F(y, k_\perp^2) = \exp\left[-\frac{(M_{MB}^2(y, k_\perp^2) - m_N^2)}{2\Lambda_{MB}^2}\right], \qquad (2)$$

where $\vec{k}_\perp$ is the transverse momentum of the meson and $M_{MB}(y, k_\perp^2)$ is the invariant mass of the intermediate two-body meson-baryon Fock state. By construction, such form factors assure the momentum sum rule [7, 12]. The parameters Λ_{MB} have been determined from an analysis of the $p \to n, \Delta, \Lambda$ fragmentation spectra [12].

The x dependence of the structure functions in the meson cloud model can be written as a sum of components corresponding to the expansion given by Eq. (1).

$$F_2^N(x) = Z\left[F_{2,\text{core}}^N(x) + \sum_{MB}\left(\delta^{(M)}F_2^N(x) + \delta^{(B)}F_2^N(x)\right)\right]. \qquad (3)$$

The contributions from the virtual mesons can be written as a convolution of the meson (baryon) structure functions and its longitudinal momentum distribution in the nucleon [13]

$$\delta^{(M)}F_2(x) = \int_x^1 dy f_M(y) F_2^M(\frac{x}{y}). \tag{4}$$

In a natural way $f_M(y)$ and $f_B(y)$ are related via [12]

$$f_B(y) = f_M(1-y). \tag{5}$$

Eq. (4) can be written in an equivalent form in terms of the quark distribution functions

$$\delta^{(M)}q_f(x) = \int_x^1 f_M(y)\, q_f^M(\frac{x}{y})\, \frac{dy}{y}. \tag{6}$$

The longitudinal momentum distributions (splitting functions, flux factors) of virtual mesons (or baryons) can be calculated assuming a model of the vertex. Further details can be found in Refs. [12].

The parton distributions "measured" in pion-nucleus Drell–Yan processes [14] are used for the mesons. The deep-inelastic structure functions of the bare baryons, $F_{2,\text{core}}^N(x,Q^2)$, $F_{2,\text{core}}^B(x,Q^2)$ are in principle unknown. Recently [16], we have extracted $F_{2,\text{core}}^N$ by fitting the quark distributions in the bare nucleon, together with (parameter-free) mesonic corrections, to the experimental data on deep-inelastic scattering. In comparison to Ref. [16] a somewhat more flexible form of the sea quark distributions in the bare nucleon has been used here. In the following we shall deal both with small and large x at relatively small Q^2, where the target mass corrections may play important role. To include the target mass corrections we follow Ref. [17] and replace the measured Bjorken-x by the target mass variable ξ [18]. In order to fix the parameters of the bare nucleon we have used the following sets of DIS data:

(a) $F_2^d(x,Q^2)$ [19],

(b) $F_2^p(x,Q^2) - F_2^n(x,Q^2)$ [19],

(c) $F_2^n(x,Q^2)/F_2^p(x,Q^2)$ [19],

(d) $F_3^{\nu N}(x,Q^2)$ [20],

The following simple parameterization has been used for the quark distributions in the bare proton at the initial scale $Q_0^2 = 4(\text{GeV}/c)^2$.

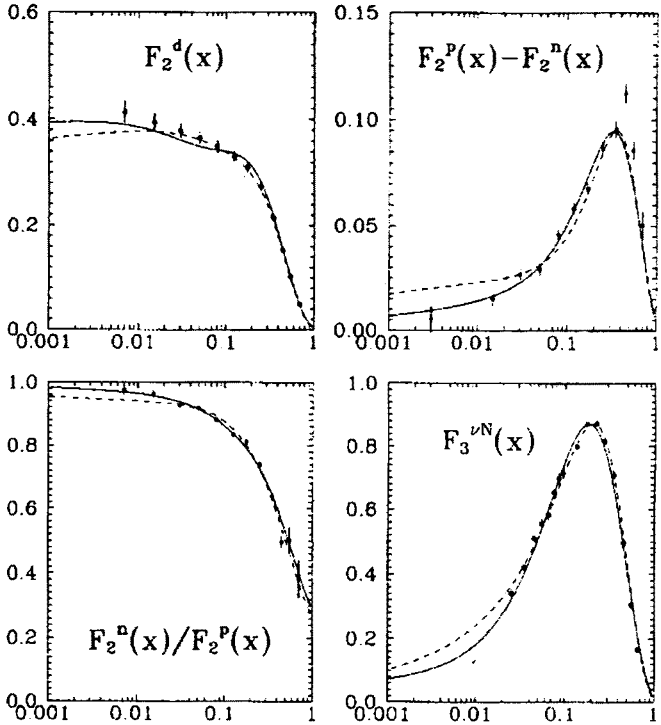

Fig. 1. The deep-inelastic scattering data. The solid line corresponds to the fit which explicitly includes the meson cloud corrections. For comparison we show result without meson cloud corrections (dashed line). (a) $F_2^d(x)$, (b) $F_2^p(x)-F_2^n(x)$, (c) $F_2^n(x)/F_2^p(x)$, (d) $F_3^{\nu N}(x)$.

$$xu_{v,\mathrm{core}}(x) = A_u x^{\alpha_u}(1-x)^{\beta_u}(1+\gamma_u x) \tag{7}$$
$$xd_{v,\mathrm{core}}(x) = A_d x^{\alpha_d}(1-x)^{\beta_d}(1+\gamma_d x) \tag{8}$$
$$xS_{\mathrm{core}}(x) = A_S(1-x)^{\eta_S}(1+\gamma_S x) \tag{9}$$
$$xg_{\mathrm{core}}(x) = A_g(1-x)^{5.3} \tag{10}$$

Note, that we have used SU(2) symmetric sea quark distribution for the bare baryons and suppressed the strange sea by a factor 2, *i.e.*

$$S_{\mathrm{core}} = u_{s,\mathrm{core}} = \overline{u}_{s,\mathrm{core}} = d_{s,\mathrm{core}} = \overline{d}_{s,\mathrm{core}} = 2s_{s,\mathrm{core}} = 2\overline{s}_{s,\mathrm{core}}. \tag{11}$$

A typical fit to the data is shown in Fig. 1. The solid line corresponds to the fit, hereafter called "Model 1" for brevity, which explicitly includes the meson cloud corrections. For comparison by the dashed line we show also a result without meson cloud correction called "Model 2".

3. Flavour asymmetry of the light antiquarks and Drell–Yan processes

The presence of the meson-(baryonic core) Fock components in the nucleon wave function leads to a violation of the Gottfried Sum Rule [3]

$$\int_0^1 [F_2^p(x) - F_2^n(x)] \, \frac{dx}{x} = \frac{1}{3}. \tag{12}$$

We obtain $S_{\rm G} = 0.224$ which is consistent with the experimental result of the NMC collaboration $S_{\rm G} = 0.24 \pm 0.016$ at $Q^2 = 5$ GeV^2 [2].

Our model has to be contrasted to the solution of Ball and Forte [22] where mesons are produced radiatively via modified Altarelli-Parisi equations. Therefore their approach predicts strong dependence of $S_{\rm G}$ on the scale, in the range of intermediate Q^2. In our approach $S_{\rm G}$ is constant, at least in the leading logarithm approximation. Preliminary results of the NMC collaboration [23] seem to confirm rather our predictions, being in disagreement with the result of the Ball and Forte approach [22].

Our model gives unique predictions for the $\bar{d}$–$\bar{u}$ asymmetry which almost coincides with the asymmetry found from the fits [24] of quark distributions to the world data on deep-inelastic and Drell–Yan processes (Fig. 2).

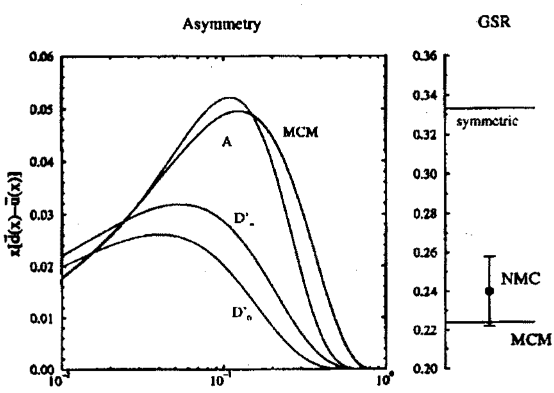

Fig. 2. The $x(\bar{d} - \bar{u})$ difference as a function of the Bjorken x calculated in our model (solid line) and compared to the newest MSR(A) [24] parameterization of the world data on DIS and Drell–Yan processes (dashed line).

A quantity which can be extracted almost directly from the experiment is

$$A_{\rm DY}(x_1,x_2)=\frac{\sigma_{pp}(x_1,x_2)-\sigma_{pn}(x_1,x_2)}{\sigma_{pp}(x_1,x_2)+\sigma_{pn}(x_1,x_2)}\ , \tag{13}$$

which we will call Drell–Yan asymmetry. In formula (13) σ_{pp} and σ_{pn} are the cross sections for the dilepton production in the proton–proton and proton–neutron scattering. Neglecting very small strange-antistrange contributions in the Drell–Yan formula the Drell–Yan asymmetry (13) can be expressed as

$$A_{\rm DY}(x_1,x_2)=\frac{[u(x_2)-d(x_2)][3\bar q(x_1)-5/2\Delta(x_1)]-[4u(x_1)-d(x_1)]\Delta(x_2)}{[u(x_2)+d(x_2)][5\bar q(x_1)-3/2\Delta(x_1)]+[4u(x_1)+d(x_1)]2\bar q(x_2)}\ , \tag{14}$$

where $\bar q=(\bar u+\bar d)/2$ and $\Delta=\bar d-\bar u$. In the case of flavour symmetric sea ($\Delta=0$), it is natural to expect that $A_{\rm DY}>0$, since $u>d$. The sign of $A_{\rm DY}$ can be, however, reversed by increasing the flavour asymmetry of the proton sea ($\Delta>0$).

The flavour asymmetry leads to a very good description of the asymmetry of the cross sections for the dilepton production in proton–proton and proton–deuteron collisions observed in the recent NA51 experiment at CERN [25] as seen in Fig. 3.

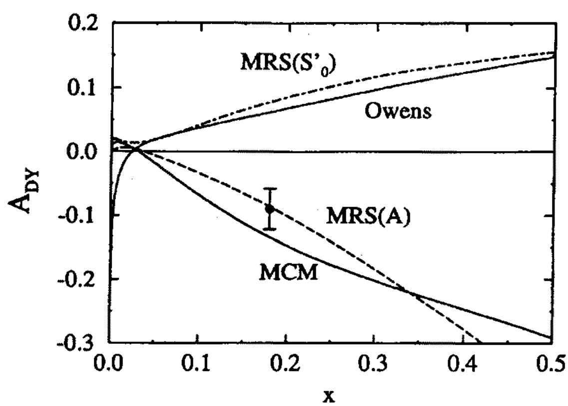

Fig. 3. The Drell–Yan asymmetry along the $x_1=x_2$ diagonal. The solid line is the result of our calculation. The experimental data point is taken from Ref. [25].

4. Properties of HERA events from DIS on pions in the proton

In deep inelastic scattering (DIS) the incident lepton is scattered on a coloured quark. Normally this results in a colour field between the struck quark and the proton remnant, such that hadrons are produced in the whole rapidity region in between. The recent discovery by the ZEUS and H1 collaborations [26] at HERA of large rapidity gap events has attracted much interest. This new class of DIS events have a large region of forward rapidity (*i.e.*close to the proton beam) where no particles or energy depositions are observed. These events have been primarily interpreted in terms of pomeron exchange.

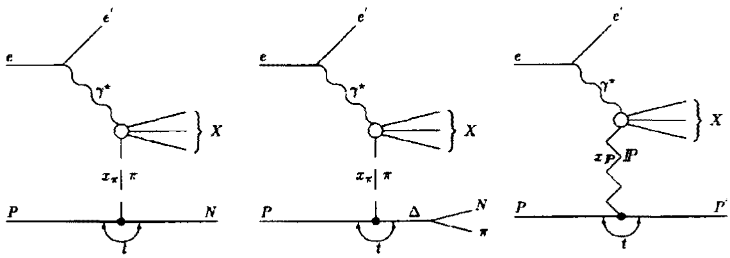

Fig. 4. Fast forward nucleon production at HERA: (a) direct production through pion-exchange, (b) indirect production via a Δ resonance in pion-exchange, (c) pomeron-exchange.

The presence of pions in the nucleon leads to an additional mechanism for nucleon production in DIS. In fixed target experiments, as (anti)neutrino deep inelastic scattering for instance, it leads to the production of slow protons. The pion-exchange model describes the proton production on a neutron target [27] (extracted from deuteron data [28]). With HERA kinematics it leads to the production of rather fast forward protons and neutrons. The mechanism is shown schematically in Fig. 4. The virtual photon 'smashes' the virtual colorless pion into debris and the nucleon (proton or neutron) or an isobar is produced as a spectator of the reaction. Therefore, the pion cloud induced mechanism could also lead to rapidity gap events. For comparison we show the pomeron-exchange mechanism in Fig. 1c.

Not only protons but also neutrons in the forward directions are interesting [29, 30]. Recently the ZEUS collaboration has installed a forward neutron calorimeter (FNCAL) [31] which will provide additional experimental information.

The cross section for the semi-inclusive spectator process $ep \to e'NX$ can be written as

$$\frac{d^4\sigma^{sp}(ep \to e'NX)}{dxdQ^2dzdp_T^2} = \frac{1}{z} f_{\pi N}(1-z,t) \frac{d\sigma^{e\pi}(x/(1-z))}{d(x/(1-z))\,dQ^2} \,. \tag{15}$$

The presence of the $\pi\Delta$ Fock component in the proton leads to the production of a spectator Δ which decays into a pion and a nucleon. The one-pion exchange contribution to the inclusive cross section can be obtained by integrating over unmeasured quantities

$$\frac{d\sigma^{ep}(x,Q^2)}{dx\,dQ^2} = \int\limits_0^{1-x} dz \int\limits_{-\infty}^{t(0,z)} dt\; f_{\pi N}(1-z,t) \frac{d\sigma^{e\pi}(x/(1-z),Q^2)}{d(x/(1-z))\,dQ^2}, \tag{16}$$

where $\sigma^{e\pi}$ is the cross section for the inclusive deep inelastic scattering of the electron from the virtual pion.

The splitting function $f(x_\pi, t)$ to the πN Fock state (Fig. 1a) is

$$f_{\pi N}(x_\pi, t) = \frac{3g^2_{p\pi^0 p}}{16\pi^2} x_\pi \frac{(-t)|F_{\pi N}(x_\pi,t)|^2}{(t-m_\pi^2)^2}, \tag{17}$$

and to the $\pi\Delta$ Fock state (Fig. 1b) is

$$f_{\pi\Delta}(x_\pi, t) = \frac{2g^2_{p\pi^-\Delta^{++}}}{16\pi^2} x_\pi \frac{(M_+^2-t)^2(M_-^2-t)|F_{\pi\Delta}(x_\pi,t)|^2}{6m_N^2 m_\Delta^2 (t-m_\pi^2)^2}, \tag{18}$$

where $M_+ = m_\Delta + m_N$ and $M_- = m_\Delta - m_N$.

The formalism presented in short above has been implemented in the Monte Carlo program POMPYT version 2.3 [32]. This program, which was originally for diffractive interactions via pomeron exchange, simulates the interaction dynamics resulting in the complete final state of particles. The basic hard scattering and perturbative QCD parton emission processes are treated based on the program PYTHIA [33] and the subsequent hadronization is according to the Lund string model [34] in its Monte Carlo implementation JETSET [33].

The main difference in comparison to the pomeron case is the replacement of the pomeron flux factor by the pion flux factors and the pomeron structure function by the pion structure function. The pion parton densities from the parametrisation GRV-P HO ($\overline{MS}$) [35] are used. If the pion-exchange mechanism is the dominant mechanism of fast neutron production, the coincidence measurement of scattered electrons and forward neutrons may allow the determination of the pion deep inelastic structure function at small x [30].

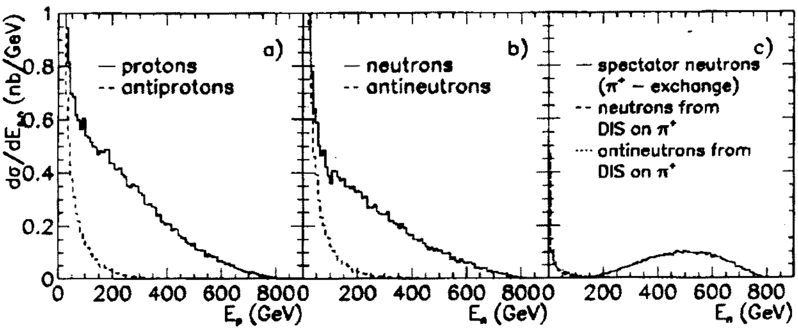

Fig. 5. Energy spectra in the HERA lab frame for nucleons ($p, \bar{p}, n, \bar{n}$) from (a,b) conventional DIS on a proton (obtained with LEPTO) and (c) DIS on an exchanged π^+ (obtained with POMPYT).

For the results presented below we have made simulations corresponding to the HERA conditions, *i.e.*26.7 GeV electrons on 820 GeV protons. The results for the pion exchange mechanism are compared with normal DIS on the proton, which is simulated with LEPTO 6.3 [36] using the MRS(D-') parton distributions [37]. In all cases, events are simulated according to the cross section formulae and are constrained to be in the kinematical region $x > 10^{-5}$, $Q^2 > 4$ GeV^2.

In Fig. 5 we show the resulting energy spectra of nucleons ($p, \bar{p}, n, \bar{n}$) in the lab frame. This is of direct interest for measurements in the leading proton spectrometer [38] and forward neutron calorimeter [31]. Neutrons from the pion exchange mechanism (panel c) have large energies giving a spectrum with a broad peak around 500 GeV, whereas the corresponding spectrum from DIS on the proton decreases monotonically with increasing neutron energy. In the region of interest, say 400–700 GeV, the two processes have a similar absolute magnitude. An observable effect from DIS on a pion should be therefore possible.

While the energy distribution of primary Δ's is very similar to that of the direct neutron production [12], after the $\Delta \to n\pi$ decay the energy distribution of the secondary nucleons becomes peaked at smaller energies of about 400 GeV [39]. The two-step mechanism is, however, much less important for the production of neutrons [40]. Therefore we concentrate on the comparison of DIS on π^+, having a neutron as spectator, with standard DIS on the proton.

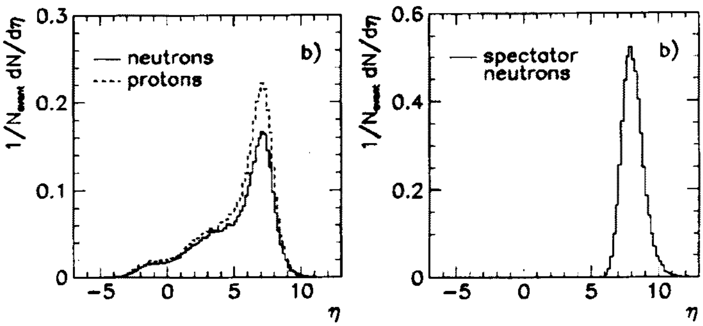

Fig. 6. Rapidity distribution of protons and neutrons from DIS on the proton as obtained from LEPTO (a) and spectator neutrons (b).

To study other characteristics of events arising through DIS on a virtual pion and compare with standard DIS on the proton, we consider spectra of different quantities normalized as

$$f(\kappa) \equiv \frac{1}{N_{\rm event}} \frac{dN}{d\kappa}\,, \tag{19}$$

where κ can be any kinematical variable and $N_{\rm event}$ is the number of events. This gives emphasis to shapes irrespectively of normalization and statistics.

A quantity with especially nice transformation properties under longitudinal boosts is rapidity which for massless particles is identical to the pseudo-rapidity defined as $\eta = -\ln\,\tan(\theta/2)$, where θ is the angle of a particle with respect to the proton beam, *i.e.*$\eta > 0$ is the proton hemisphere in the HERA lab frame.

For example in Fig. 6 I compare the pseudo-rapidity spectrum of neutrons from non-diffractive DIS (a) and the spectrum of spectator neutrons (b). The geometry of the ZEUS apparatus assures almost 100% geometrical acceptance of spectator neutrons and only about 50% for non-diffractive neutrons. This should further facilitate the identification of the interesting component.

The pseudo-rapidity variable is of particular interest in the context of large rapidity gap events. Based on our Monte Carlo simulated events using LEPTO and POMPYT we extract $\eta_{\rm max}$ (maximal pseudo-rapidity in the event) and show its distribution in Fig. 7 for conventional non-diffractive DIS on the proton, DIS on an exchanged π^+ and diffractive DIS on a pomeron. From this model study we find a shift of about one unit towards smaller $\eta_{\rm max}$ in case of DIS on the pion as compared to normal DIS.

For the spectrum of $\eta_{\rm max}$ for DIS on the pomeron, we have taken a set of parameters which is usually called 'hard pomeron' in the literature.

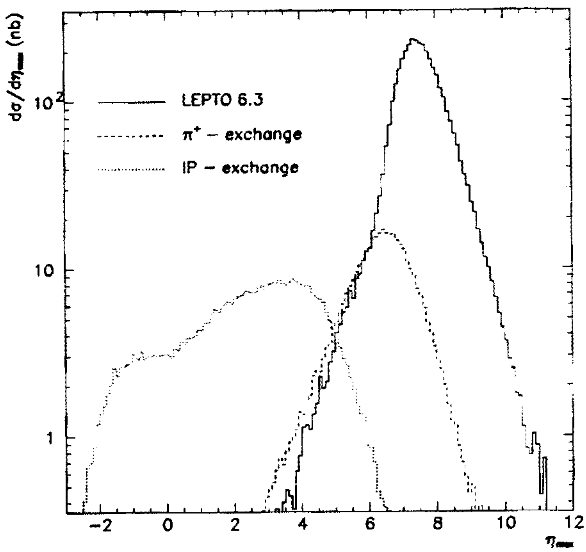

Fig. 7. Distribution of $\eta_{\rm max}$ (see text) in non-diffractive DIS on the proton (solid), in DIS on the virtual π^+ (dashed) and in DIS on the pomeron (dotted).

The pomeron is assumed to contain equal amounts of the light quarks, *i.e.* $u = \bar{u} = d = \bar{d}$, each with a density distribution $zq(z) = \frac{6}{4}z(1-z)$, with the normalization chosen such that the parton distributions fulfill the momentum sum rule. The pomeron flux factor is here taken as the ratio of the single diffractive cross section and the pomeron-proton total cross section [41]. The resulting $\eta_{\rm max}$ distribution from DIS on the pomeron is considerably different from the other two cases.

From Fig. 7 one may conclude that the pion–exchange induced DIS leads to events with intermediate size rapidity gaps rather than to those with large gaps. Nonetheless it is important to verify experimentally the effect of the pion exchange by, *e.g.*, correlating $\eta_{\rm max}$ with fast forward neutrons measured in FNCAL.

The flux factor given by Eq. (17) with a cut-off parameter of the vertex form factor extracted from the high-energy neutron production data [12] predicts that the pion carries, on average, a fraction 0.3 of the proton beam momentum [43]. This implies that as a first approximation the pion-induced DIS processes can be viewed as an electron scattering on the pion with effective energy $E_{\rm eff} \approx 0.3 \cdot E_{\rm beam}$. Because of the smaller energy of the pion one could expect smaller multiplicity of electron-pion DIS events in comparison to those for the electron-proton DIS. In Fig. 8 we compare the model predictions of the multiplicity spectra for DIS on the proton with

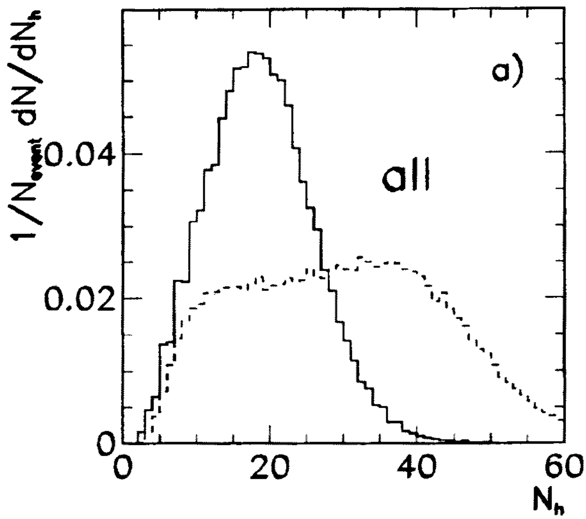

Fig. 8. Multiplicity distributions of all stable particles from DIS on a π^+ (full curves) and DIS on a proton (dashed curves).

those on π^+. The multiplicities in DIS events on the pion is noticeably smaller than in DIS events on the proton; the average multiplicity is about 20 and 30, respectively. However, due to the large fluctuations in multiplicity and the overlap between the distributions for the two cases, as well as the distortions that limited experimental acceptance will create, it is not clear whether this difference can be used as a discriminator.

5. Production of the W and Z bosons in the nucleon–(anti)nucleon collisions

In the leading order (LO) approximation in the framework of improved parton model [44] the total $B(= W^{\pm}, Z^0)$ boson cross section is the convolution of elementary cross section $\hat{\sigma}(q\bar{q}' \to B)$ with the quark densities

$$\begin{aligned}\sigma(h_1h_2 \to BX) \; &= \; \frac{K}{3}\int_0^1 dx_1dx_2\sum_{q,q'} \\ &\Big[q(x_1, M_B^2)\,\bar{q}'(x_2, M_B^2)\,\hat{\sigma}(q\bar{q}' \to B) \\ &+\bar{q}'(x_1, M_B^2)\,q(x_2, M_B^2)\,\hat{\sigma}(\bar{q}'q \to B)\Big]\,. \qquad (20)\end{aligned}$$

In analogy to the Drell–Yan processes the so-called K-factor in Eq. (20) includes first order QCD corrections [44]). The elementary cross sections in

(20) can be easily calculated within the Standard Model [44]. Then the rapidity distribution of $W^{\pm}$ boson produced in the h_1+h_2 collision is

$$\frac{d\sigma}{dy_W}(h_1 h_2 \to W^{\pm} X) =$$
$$K\,\frac{2\pi G_F}{3\sqrt{2}}\,x_1 x_2 \sum_{q,q'} |V_{qq'}|^2 \Big[q(x_1, M_W^2)\,\bar{q}'(x_2, M_W^2)$$
$$+\bar{q}'(x_1, M_W^2)\,q(x_2, M_W^2)\Big]\,. \tag{21}$$

In analogy the rapidity distribution for Z^0 boson is

$$\frac{d\sigma}{dy_Z}(h_1 h_2 \to Z^0 X) =$$
$$K\,\frac{8\pi G_F}{3\sqrt{2}}\,x_1 x_2 \sum_q [(g_V^q)^2 + (g_A^q)^2]$$
$$\times\Big[q(x_1, M_Z^2)\,\bar{q}(x_2, M_Z^2) + \bar{q}(x_1, M_Z^2)\,q(x_2, M_Z^2)\Big]\,. \tag{22}$$

In Eq. (21) and (22) the quark distributions must be evaluated at $x_{1/2} = \frac{M_B}{\sqrt{s}} e^{\pm y_B}$, where $B = W$ or Z.

The formulae for the differential cross sections for the production of charged leptons from $W^{\pm}$ and Z decays are somewhat cumbersome and will be presented in detail in Ref. [45]. In practical calculations we shall use $M_W = 80.22$ GeV, $mit\Gamma_W = 2.08$ GeV and $M_Z = 91.173$ GeV, $\Gamma_Z = 2.487$ GeV [46].

The calculation of the cross sections for the gauge boson production (Eq. (21) and (22)) or the cross section for the lepton from the gauge boson decay requires parton distributions at $Q^2 = M_W^2(M_Z^2)$. For this purpose the parton distributions found in Section 2 have been evolved by the Gribov–Lipatov–Altarelli–Parisi (GLAP) evolution equations [47].

The ambiguity due to the uncertainty in α_s practically cancels below $s^{1/2} = 1.2$ TeV and becomes important only at larger $s^{1/2}$. In Table I we compare the total cross sections obtained in our model multiplied with corresponding branching ratio $BR(W^{\pm} \to e^{\pm}\nu(\bar{\nu}))$, $BR(Z^0 \to e^+e^-)$, with those measured at CERN and Fermilab. In the heavy top-quark approximation $BR(W^{\pm} \to e^{\pm}\nu(\bar{\nu})) \approx \frac{1}{9}$ and $BR(Z^0 \to e^+e^-) \approx \frac{1-4x_W+8x_W^2}{21-40x_W+\frac{160}{3}x_W^2}$. A reasonable agreement of the total cross sections obtained within our model with those measured by UA1 [48], UA2 [49, 50] and CDF [51, 52] collaborations can be seen. Since in the present paper we shall be interested mainly in relative effects (ratios, asymmetries), where the ambiquity due to the QCD evolution cancels almost completely, hereafter we shall limit to $\Lambda^{(4)}_{\rm QCD} = 200$ MeV.

TABLE I

The total cross sections times branching ratio $\sigma_{\rm tot}(p\bar{p} \to W^{\pm}X) \cdot BR(W^{\pm} \to e^{\pm}\nu(\bar{\nu}))$, $\sigma_{\rm tot}(p\bar{p} \to Z^0X) \cdot BR(Z^0 \to e^+e^-)$ (in nb) for the production of W and Z bosons at CERN (upper block) and Fermilab (lower block).

boson	model 1	model 2	Owens	GRV95(LO)	experiment
$W^+ + W^-$	750.6	751.4	795.2	736.0	682 ± 12 ± 40 [50]
Z	71.7	68.2	74.5	70.0	65.6 ± 4.0 ± 3.8 [50]
$W^+ + W^-$	2548.0	2558.0	2298.0	2534.0	2200 ± 200 [52]
Z	234.1	233.1	218.6	236.6	214 ± 23 [52]

Naively one would expect that the total cross section for the production of gauge W bosons should be smaller in the proton–proton collisions than in the proton–antiproton collisions, because in the latter case the antiproton is an efficient donor of antiquarks. This was used in the past as a strong argument for the construction of proton–antiproton colliders such as those at CERN and Fermilab. Since at that time it was strongly believed that the nucleon sea is symmetric with respect to the light flavours, no $\bar{d} \neq \bar{u}$ scenario has been considered. At present there are fairly convincing arguments [25, 16] for the $\bar{d}$–$\bar{u}$ asymmetry. Can the $\bar{d}$–$\bar{u}$ asymmetry induced by the meson cloud in the nucleon modify this simple expectation? In Fig. 9 we compare the proton–proton and proton–antiproton cross sections for

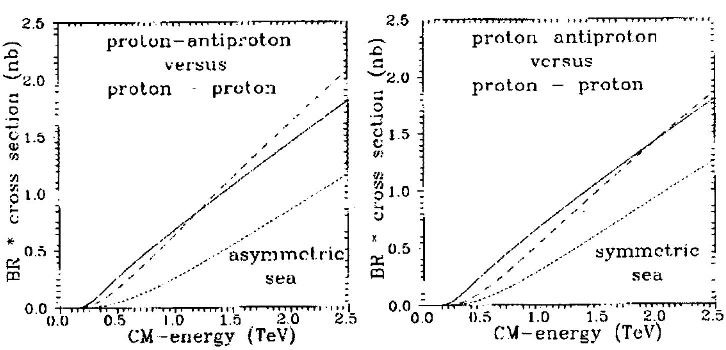

Fig. 9. A comparison of the total cross sections for the production of W-boson in the proton–proton (solid) and proton–antiproton (dashed) collisions. In panel (a) we show the results for the asymmetric sea induced by the meson cloud and in panel (b) the results for the symmetric sea quark parametrization.

the "asymmetric" (panel b) and "symmetric" (panel a) cases. The corresponding cross sections are denoted as: $\sigma_{\rm tot}(p\bar{p} \to W^+) = \sigma_{\rm tot}(p\bar{p} \to W^-)$ (solid), $\sigma_{\rm tot}(pp \to W^+)$ (dashed) and $\sigma_{\rm tot}(pp \to W^-)$ (dotted). As expected, without meson cloud, with symmetric sea quark distributions, the cross section for the production of W^+ is smaller in the proton–proton case than in the proton–antiproton case. In contrast, much larger cross sections are obtained if the meson cloud effects are included (see panel a). As seen from the figure, in the broad range of energy $\sigma_{\rm tot}(pp \to W^+) > \sigma_{\rm tot}(p\bar{p} \to W^+) = \sigma_{\rm tot}(p\bar{p} \to W^-)$. A huge enhancement of the cross section due to the meson cloud effects close to the threshold can be observed in the proton–proton collision case. In principle this effect could be studied in the future at the heavy-ion collider RHIC. There is practically no such enhancement in the proton–antiproton collision case [45], except very close to the threshold, where the corresponding cross section is negligibly small.

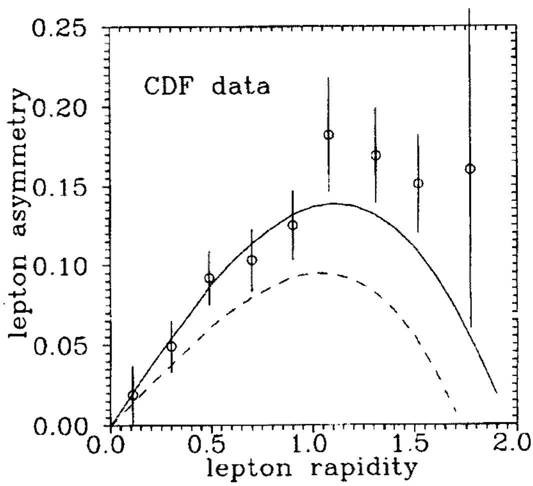

Fig. 10. Predictions for the asymmetry $A_{p\bar{p}}^{e^+e^-}$ of the rapidity distributions of the charged leptons from the $W^\pm \to l^\pm \nu$ decays in the proton–antiproton collisions. Shown are results of Model 1 (solid) and Model 2 (dashed).

A very interesting quantity is the asymmetry of charged leptons from $W^\pm \to l^\pm(\nu,\bar{\nu})$ decays defined as

$$A_{p\bar{p}}^{l^+l^-}(y_l) = \frac{\frac{d\sigma}{dy_l}(p\bar{p} \to W^+X \to l^+\tilde{X}) - \frac{d\sigma}{dy_l}(p\bar{p} \to W^-X \to l^-\tilde{X})}{\frac{d\sigma}{dy_l}(p\bar{p} \to W^+X \to l^+\tilde{X}) + \frac{d\sigma}{dy_l}(p\bar{p} \to W^-X \to l^-\tilde{X})}\,. \quad (23)$$

The quantity has been measured recently by the CDF collaboration at the Fermilab $p\bar{p}$ Tevatron collider [53, 54]. In Fig. 10 I show the experimental result together with results of different calculations. The experimental data have been folded across $y_l = 0$ [54] based on the CP invariance. In the calculation experimental cut [54] $p^l_{T,\min} = 25$ GeV has been applied. We show both asymmetries obtained in our Model 1 (solid line) and Model 2 (dashed line). As clearly seen from the figure the presence of the meson cloud considerably improves the agreement with the experimental asymmetry. A similar quality agreement with the CDF asymmetry has been achieved recently in Ref. [55] where the quark distributions from Ref. [56] have been used. While in Ref. [56] the $\bar{d}$–$\bar{u}$ asymmetry was introduced purely phenomenologically, in the present paper the $\bar{d}$–$\bar{u}$ asymmetry is ascribed to the effects caused by the meson cloud in the nucleon.

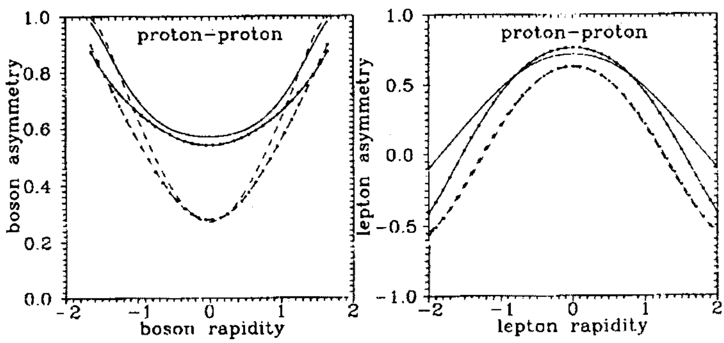

Fig. 11. $A_{pp}^{W^+W^-}$ (panel a) and corresponding $A_{pp}^{e^+e^-}$ (panel b). The asymmetries obtained in Model 1 (solid line) and Model 2 (dashed line) are compared with the results obtained with the GRV95(LO) parametrization [56] (solid line with dots) and the Owens parametrization [59] (dashed line with dots).

Having shown that our parton distributions lead to good description of DIS data at relatively low Q^2 and describe the gauge bosons production data in the proton–antiproton collisions fairly well, we shall try to make some interesting predictions for the W/Z production in nucleon–nucleon collisions, which could be measured in principle at the future collider RHIC originally designed to study the quark-gluon plasma in heavy ion – heavy ion collisions. In the following we shall fix the energy $s^{1/2}$ to 500 GeV which could be roughly adequate for the proton–proton collisions at RHIC. In Fig. 11 I present $A_{pp}^{W^+W^-}$ (panel a) and in analogy to the proton–antiproton case $A_{pp}^{e^+e^-}$ (panel b). Let us demonstrate that the $A_{pp}^{W^+W^-}$ is a quantity sensitive to the $\bar{u}$–$\bar{d}$ asymmetry. For this purpose let us write

$$\bar{u}(x,Q^2) = S(x,Q^2) - \frac{\Delta(x,Q^2)}{2} \quad , \quad \bar{d}(x,Q^2) = S(x,Q^2) + \frac{\Delta(x,Q^2)}{2} \,. \tag{24}$$

Then taking $y_W \approx 0$ ($x_1 \approx x_2$) and neglecting small (Cabbibo suppressed) contributions from the strange quarks, the asymmetry $A_{pp}^{W^+W^-}$ can be written as

$$A_{pp}^{W^+W^-}(x) \approx \frac{R_v(x)\, S(x) + \frac{\Delta(x)}{2}}{S(x) + R_v(x)\, \frac{\Delta(x)}{2}}\,, \tag{25}$$

where we have introduced $R_v(x) \equiv \frac{u_v(x)-d_v(x)}{u_v(x)+d_v(x)}$ for brevity. Eq. (25) clearly demonstrates the sensitivity to the $\bar{u}$–$\bar{d}$ asymmetry which in our model is due to the meson cloud. The sensitivity to the $\bar{u}$–$\bar{d}$ difference can be better visualized in

$$R_{pp}^{W^+W^-} \equiv \frac{\sigma(pp \to W^+X)}{\sigma(pp \to W^-X)} \approx \frac{u(x, M_W^2)}{d(x, M_W^2)} \cdot \frac{\bar{d}(x, M_W^2)}{\bar{u}(x, M_W^2)}\,. \tag{26}$$

The first ratio is known fairly well from the CDF data (see for instance [24]). Therefore the measurement of $R_{pp}^{W^+W^-}(x = \frac{M_W}{\sqrt{s}})$ in p+p collision should give an accurate determination of the ratio $\frac{\bar{d}(x,M_W^2)}{\bar{u}(x,M_W^2)}$. For a typical RHIC energy $s^{1/2} = 500$ GeV, $x \approx 0.16$. This is a region of sizeable $\bar{u}$–$\bar{d}$ asymmetry. Analogous ratio has been determined recently at $Q^2 \approx 20$ GeV^2 from the measurement of Drell–Yan asymmetry in proton–proton and proton–deutron collisions by the NA51 experiment at CERN [25]. There, however, the $\frac{\bar{u}(x)}{\bar{d}(x)}$ is biased by the explicit assumption about proton–neutron isospin symmetry [16]. In contrast $R_{pp}^{W^+W^-}(x)$ is free of such an assumption.

In Ref. [45] we shall study different similar asymmetries possible to measured in the proton–proton and proton–deuteron collisions which would be of great help in studying the asymmetry of the sea quark distributions in the nucleon. Whether such an analysis will be possible in the future at the heavy-ion collider RHIC requires new studies of several experimental aspects.

6. Conclusions

The concept of a pion cloud in the nucleon was recently found to be very useful in understanding the Gottfried sum rule violation observed by the New Muon Collaboration [2] and the Drell–Yan asymmetry measured recently in the NA51 Drell–Yan experiment at CERN [25]. We have investigated several quantities in order to find useful observables which would help to verify this concept using deep inelastic electron-proton scattering at HERA. We have therefore analyzed the structure of deep inelastic events induced by the pion-exchange mechanism. In particular, we have studied distributions of final nucleons as well as rapidity and multiplicity spectra. Most of the event characteristics do not provide a direct possibility to distinguish the events from DIS on a pion from the ordinary events with DIS on a proton. A clear difference is, however, found in the energy spectrum of outgoing neutrons. We find that the pion cloud model predicts an energy distribution of neutrons which substantially differs from the standard hadronization models. While the pion-exchange mechanism leads to an energy spectrum which peaks at an energy of about $0.7E_{\mathrm{beam}}$, *i.e.*at about 500 GeV, the spectrum of neutrons produced in the standard hadronization process following DIS on the proton decreases monotonically with increasing neutron energy. This should facilitate to discriminate between the two processes.

We have shown that the pion cloud induced mechanism practically does not contribute to the large rapidity gap events observed recently by the ZEUS and H1 collaborations [26] and cannot be a severely competing mechanism for the pomeron exchange. The multiplicity of the pion cloud induced events is about 60-70% of that for standard hadronization on the proton, but given the large fluctuations it is not clear to what extent this difference can be exploited.

We have investigated also possible effects of the meson cloud in the nucleon on the production of weak gauge bosons in proton–antiproton, proton–proton and proton–deuteron collisions.

A reasonable agreement of the total cross sections with those measured at CERN by the UA1 [48], UA2 [49, 50] collaborations and at Fermilab by the CDF [51, 52] collaboration has been obtained. If the meson cloud effects are included in the broad range of energy $\sigma_{\mathrm{tot}}(pp \to W^-) > \sigma_{\mathrm{tot}}(p\bar{p} \to W^+) = \sigma_{\mathrm{tot}}(p\bar{p} \to W^-)$, in contrast to naive expectations. In contrast to parton distributions with SU(2) symmetric sea we find a good description of the charged lepton asymmetry measured recently by the CDF collaboration [54] which may be treated as an indirect evidence of the meson cloud in the nucleon.

We have analysed some asymmetries of the cross sections for the production of W/Z bosons in the proton–proton and proton–deuteron collisions. We find that such observables can be very useful to shed new light on the problem of the $\bar{d}$–$\bar{u}$ asymmetry in the nucleon. These quantities could in principle be studied in the future at the heavy ion collider RHIC. Whether such an analysis will be possible in practice will require, however, new studies of several experimental aspects.

In future, lattice QCD calculation should address quantitatively the problem of the pion (meson) cloud. At present the lattice QCD calculation gave only some qualitative evidence for the importance of pion loop effects for nucleon properties [57]. Some authors discuss the pionic dressing of the constituent quarks in the nucleon [58], which is also capable of generating the $\bar{u}$-$\bar{d}$ asymmetry. In contrast to our approach these models are, however, unable to make any link to high-energy production of baryons.

I wish to thank M. Ericson, H. Holtmann, G. Ingelman, N.N. Nikolaev, M. Przybycień, J. Speth and V. Uleshchenko for collaboration on issues presented here.

REFERENCES

[1] D.A. Ross, C.T. Sachrajda, *Nucl. Phys.* **B149**, 497 (1979).
[2] P. Amaudruz *et al.*, *Phys. Rev. Lett.* **66**, 2712 (1991).
[3] K. Gottfried, *Phys. Rev. Lett.* **18**, 1174 (1967).
[4] E.M. Henley, G.A. Miller, *Phys. Lett.* **B251**, 453 (1990).
[5] A. Signal, A.W. Schreiber, A.W. Thomas, *Mod. Phys. Lett.* **A6**, 271 (1991).
[6] W-Y.P. Hwang, J. Speth, G.E. Brown, *Z. Phys.* **A339**, 383 (1991).
[7] V.R. Zoller, *Z. Phys.* **C53**, 443 (1992).
[8] A. Szczurek, J. Speth, *Nucl. Phys.* **A555**, 249 (1993).
[9] A. Szczurek, H. Holtmann, *Acta Phys. Pol.* **B24**, 1833 (1993).
[10] A. Szczurek, J. Speth, G.T. Garvey, *Nucl. Phys.* **A570**, 765 (1994).
[11] N.N. Nikolaev, A. Szczurek, J. Speth, V. Zoller, *Z. Phys.* **A349**, 59 (1994).
[12] H. Holtmann, A. Szczurek, J. Speth, *Nucl. Phys.* **A596**, 631 (1996).
[13] J.D. Sullivan. *Phys. Rev.* **D5**, 1732 (1972).
[14] P.J. Sutton, A.D. Martin, R.G. Roberts, W.J. Stirling, *Phys. Rev.* **D45**, 2349 (1992).
[15] W.-Y.P. Hwang, J. Speth, *Phys. Rev.* **D46** 1198 (1992).
[16] A. Szczurek, M. Ericson, H. Holtmann, J. Speth, *Nucl. Phys.* **A596**, 397 (1996).
[17] A.D. Martin, W.J. Stirling, R.G. Roberts, *Phys. Rev.* **D51**, 4756 (1995).
[18] A.de Rujula, H. Georgi, H.D. Politzer, *Ann. Phys. (N.Y.)* **109**, 315 (1977).
[19] M. Arneodo *et al.*, *Phys. Rev.* **D50**, R1 (1994).
[20] W.C. Leung, *Phys. Lett.* **B317**, 655 (1993).
[21] S.R. Mishra, *Phys. Rev. Lett.* **68**, 3499 (1992).
[22] R.D. Ball, S. Forte, *Nucl. Phys.* **B425**, 516 (1994).
[23] A. Brüll, Habilitationsschrift, Heidelberg 1995.
[24] A.D. Martin, W.J. Stirling, R.G. Roberts, *Phys. Rev.* **D50**, 6734 (1994).
[25] A. Baldit *et al.*, *Phys. Lett.* **B332**, 244 (1994).
[26] ZEUS Collaboration, M. Derrick *et al.*, *Phys. Lett.* **B315**, 481 (1993); H1 Collaboration, T. Ahmed *et al.*, *Nucl. Phys.* **B429**, 477 (1994).
[27] A. Szczurek, G.D. Bosveld, A.E.L. Dieperink, *Nucl. Phys.* **A595**, 307 (1995).

[28] G.D. Bosveld, A.E.L. Dieperink, A.G. Tenner, *Phys. Rev.* **C49**, 2379 (1994).
[29] G. Levman, K. Furutani, Virtual Pion Scattering at HERA, ZEUS note 92(1992); G. Levman, K. Furutani, A Forward Neutron Calorimeter for ZEUS, DESY-PRC 93-08 (1993).
[30] H. Holtmann, G. Levman, N.N. Nikolaev, A. Szczurek, J. Speth, *Phys. Lett.* **B338**, 363 (1994).
[31] S. Bhadra *et al.*, *Nucl. Instrum. Methods* **A354**, 479 (1995).
[32] P. Bruni, G. Ingelman, POMPYT 2.3 – A Monte Carlo to Simulate Diffractive Hard Scattering Processes, unpublished program manual.
[33] T. Sjöstrand, PYTHIA 5.7 and JETSET 7.4, CERN-TH.7112/93 and Comput. Phys. Commun. **82**, 74 (1994).
[34] B. Andersson, G. Gustafson, G. Ingelman, T. Sjöstrand, *Phys. Rep.* **97**, 31 (1983).
[35] M. Glück, E. Reya, A. Vogt, *Z. Phys.* **C53**, 651 (1992).
[36] G. Ingelman, LEPTO 6.3, unpublished manual, see also G.Ingelman, LEPTO 6.1, Proc. of the DESY Workshop "Physics at HERA" Ed. W. Buchmüller and G. Ingelman, Hamburg, 1366 (1991).
[37] A.D. Martin, R.G. Roberts, W.J. Stirling, *Phys. Lett.* **B306**,145 (1993).
[38] The ZEUS detector, status report, DESY 1993.
[39] H. Holtmann, N.N. Nikolaev, A. Szczurek, J. Speth, B.G. Zakharov, *Z. Phys.* **C69**, 297 (1996).
[40] M. Przybycień, A. Szczurek, G. Ingelman, DESY 96-073, submitted to *Z. Phys.* **C**.
[41] G. Ingelman, P. Schlein, *Phys. Lett.* **B152**, 256 (1985).
[42] E.L. Berger, J.C. Collins, D.E. Soper G. Sterman, *Nucl. Phys.* **B286**, 704 (1987).
[43] H. Holtmann, A. Szczurek, J. Speth, Preprint KFA-IKP(TH)-1993-33.
[44] V.D. Barger, R.J.N. Philips, *Collider Physics*, Addison-Wesley Pub. Com., Redwood City 1987.
[45] A. Szczurek, V. Uleshchenko, H. Holtmann, J. Speth, paper in preparation.
[46] Review of Particle Properties, *Phys. Rev.* **D45**, 1 (1992).
[47] G. Altarelli, G. Parisi, *Nucl. Phys.* **B126**, 298 (1977).
[48] C. Albajar *et al.*, (UA1 Collaboration), *Phys. Lett.* **B253**, 503 (1991).
[49] J. Alitti *et al.*, (UA2 Collaboration), *Z. Phys.* **C47**, 11 (1990).
[50] J. Alitti *et al.*, (UA2 Collaboration), *Phys. Lett.* **B276**, 365 (1992).
[51] F. Abe *et al.*, (CDF Collaboration), *Phys. Rev.* **D44**, 29 (1991).
[52] F. Abe *et al.*, (CDF Collaboration), *Phys. Rev. Lett.* **69**, 28 (1992).
[53] F. Abe *et al.*, (CDF Collaboration), *Phys. Rev. Lett.* **68**, 1459 (1992).
[54] F. Abe *et al.*, (CDF Collaboration), *Phys. Rev. Lett.* **74**, 850 (1995).
[55] S. Kretzer, E. Reya, M. Stratmann, *Phys. Lett.* **B348**, 628 (1995).
[56] M. Glück, E. Reya, A. Vogt, *Z. Phys.* **C67**, 433 (1995).
[57] T.D. Cohen, D.B. Leinweber, *Comments Nucl. Part. Phys.* **21**, 137 (1993).
[58] E. Eichten, I. Hinchliffe, C. Quigg, *Phys. Rev.* **D45**, 2269 (1992).
[59] J.F. Owens, *Phys. Lett.* **B266**, 126 (1991).